



NON-LINEAR DYNAMICS TOOLS FOR THE MOTION ANALYSIS AND CONDITION MONITORING OF ROBOT JOINTS

I. TREDAFILOVA AND H. VAN BRUSSEL

Department of Mechanical Engineering, Katholieke Universiteit Leuven, Leuven, Belgium.

E-mail: irina.trendafilova@mech.kuleuven.ac.be

(Received 29 February 2000, accepted 20 December 2000)

Time series from non-damaged and three types of damaged robot joints are considered and analysed from the viewpoint of non-linear dynamics. The embedding spaces for the four types of signals are recovered. The application of surrogate data tests is used to prove the presence of non-linearities in the joints. The results suggest a rise in unstable behaviour due to the introduction of backlash in robot joints. The chaotic behaviour gets stronger with the increase of the backlash extent. This is confirmed by the increase of the embedding dimension as well as by the increase of the Lyapunov exponents and the correlation dimension with the backlash increase. A straightforward method for condition monitoring using non-linear dynamics characteristics, based on a classification procedure, is suggested.

© 2001 Academic Press

1. INTRODUCTION

The dynamics of a robot joint is commonly rather complex. Some phenomena to be taken into account are friction, deformation of non-linear materials, geometry of the part, dynamics and geometry of the other parts connected to the joint. In general, robot joints demonstrate non-linear dynamic behaviour, which can be due to a number of different reasons and is caused by different mechanisms. The presence of non-linearities and the consequent non-linear behaviour exhibited by robot parts is a problem that gives rise to serious difficulties in the kinematic and especially the dynamic modelling, analysis and control of robot joints. It becomes rather difficult to develop an accurate model that takes into account the different phenomena (like friction, joint and link flexibility, backlash and clearances) that influence the system dynamics. The non-linear behaviour poses serious difficulties in the process of the analysis of signals recorded from different elements and in the related inverse dynamic problems, i.e. identification and control which are rather important for the design and analysis of robotic structures and their components.

In this paper, we use the data dependent approach to analyse the behaviour of robot joints, for several cases when a backlash is present as well as for the case of no backlash, from the standpoint of non-linear dynamics, making use of the recorded acceleration signals. The approach is based on the assumption that a backlash introduces a non-linearity in the joint. Thus, in all cases when backlash is present in the joint we are dealing with non-linear motion. Accordingly, the non-linear motion invariants are supposed to change with the change of the backlash size. Then the non-linear invariants might be employed to generate features from the recorded signals and use them for backlash detection and quantification. All these assumptions are proved by using the time data from the response acceleration signals. We first analyse the behaviour of robot connections when different

backlash is present and in the state of no backlash starting from their time responses, spectra and using pseudo-phase-space representations. The next step is to recover the embedding space necessary to unfold the motion for all the types of joints considered. This includes the determination of the time lag and the embedding dimension. We further try to establish the kind of dynamic behaviour for all the categories of joints we introduce using surrogate data tests. As will be demonstrated later, for the robot joints despite the periodic behaviour of the arm, there is another component which makes the motion definitely non-linear, especially when looking at a single transient. We prove that this component is a non-linear deterministic one. Thus a non-linear deterministic model for the dynamic behaviour of robot joints can be recovered. Unfolding their dynamics and recovering the embedding time delay space is the first step towards reconstructing a model. By using the recovered embedding state space, we are now able to more accurately estimate some of the motion invariants for all the joint types. The consequent determination of some non-linear (chaotic) dynamics invariants (Lyapunov exponents, attractor dimensions) confirms some conclusions, already suggested from the previous analysis. The obtained Lyapunov exponents suggest the degree of chaoticity for the considered signals. They prove the conclusions, already implied by the surrogate data tests: there is weak chaoticity in the cases of no backlash and small backlash and the degree of chaoticity increases with the increase of the backlash size. Ultimately, the reconstruction of the unfolding space can be used for building local and global models of the dynamics of the system. Such kinds of models can be utilised to develop procedures for defect qualification and quantification, applying inverse identification methods.

Another problem that is considered in the paper is the application of the obtained non-linear dynamics results for the purpose of robot joints condition monitoring. Early defect detection in robot connections is another very important issue that is pursued extensively due to its significance for a lot of practical applications. The dynamic response of robot joints is influenced by the condition of the links. The presence of even a small defect causes changes in the measured dynamic signature. Accordingly, defects of different types and sizes induce different vibration signals. The dynamic response of structures is widely accepted and used for purposes of fault detection and quantification. This paper offers a straightforward procedure for condition monitoring of robot joints, based on their non-linear dynamics characteristics. As was expected, the non-linear dynamics invariants prove to change with the backlash size. The obtained results are used to develop a condition monitoring method for robot joints with a backlash that uses some non-linear dynamics characteristics. A classifier is built to demonstrate its application.

2. STATE-OF-THE-ART

Non-linear dynamic systems have attracted a lot of attention during the last couple of decades. The non-linear behaviour can be caused by a local (friction, backlash, clearances) or global (material non-linear behaviour, large deformations, buckling, kinematic non-linearities) non-linearity. It became clear that most methods used for the analysis and characterisation of linearly behaving dynamic systems are not applicable in a lot of cases of non-linear behaviour. A lot of research was done that was directed towards modelling, identification and detection of non-linearities in dynamic systems [1–12].

Sometimes, for a number of application purposes it is important to know whether a linear approach should be valid for a certain dynamic system. Therefore, a lot of effort was put into the development of different detection techniques. Some detection procedures look for distortions in the frequency response functions (FRFs) of the system [1–4]. The application of the Hilbert transform (HT) in the frequency domain can be used as a sensitive diagnostic

for detecting non-linear dynamic behaviour [1, 2, 7]. A lot of detection procedures are based on dissimilarity measures between the signals coming from a linear system and the system under test in the time or the frequency domain [1, 2, 5, 6, 7]. Although detection is an important step, it should be kept in mind that the final goal is the identification of a valid and accurate enough model of the system under test.

For a lot of theoretical as well as practical purposes, like simulation, prediction, design and control, a valid mathematical model of the characteristic behaviour of the system is needed. Such a model can be derived in different ways. The most popular approaches especially for non-linear systems use identification methods and are based on the input/output measurements in the time or the frequency domain. The HT over the time domain proved useful for purposes of identification. It can be used to characterise and classify the responses of non-linearly behaving systems [2, 6]. In general, for a non-linear system the FRFs are excitation dependent, which poses difficulties in their application for modal analysis [1, 2, 5, 6, 9]. The use of functional series—Volterra and Wiener series—for analysis and characterisation of non-linear systems has been extensively developed and applied for different applications [1, 2, 9]. They propose an idea for higher order resonance plots, which provide information about non-linear transfer of energy between frequencies. They also propose a form of ‘hypermodal’ analysis where non-linear structural parameters are extracted from higher-order FRFs. The use of the experimentally estimated higher-order FRFs for the characterisation of non-linearly behaving dynamic systems presents to be promising and very useful in some aspects of techniques, because they offer a well-known identification tool applicable for multiple dof systems and since no *a priori* information about the system is needed. However, their application poses some difficulties, mainly that some common types of non-linearities cannot be satisfactorily described. An approach which has recently gained a lot of popularity and proved rather successful for single as well as for multiple dof systems is the application of the Karhunen–Loeve transform [4, 5, 6, 8, 9]. It is also known as the proper orthogonal decomposition and is being recently explored for determining normal modes for non-linearly behaving systems as well as for the purposes of detection and identification [2, 4, 8, 9]. It is a statistical pattern analysis technique for finding the dominant structures in an ensemble of spatially distributed data. It is used to create lower-order models for systems with non-linearities. Then, the singular value decomposition procedures can be used to compute the modal metrics and the proper orthogonal modes for a non-linear system. The proper orthogonal modes can be shown to converge to the normal modes under some circumstances [5, 8]. Another technique, taken from the linear theory and extended for the non-linear case, is the use of autoregressive (AR) and autoregressive moving average (ARMA) models [1, 2, 9]. There are numerous attempts to generalise the model structure to the non-linear case [9]. Different NARMA models have been developed and proposed for different systems for the purposes of modelling and identification [2, 9]. Normally, the success of such models depends on the system under investigation and the type and the order of the chosen model. The application of artificial neural networks (ANN) for the purposes of modelling and identification purposes should also be noted [10–13]. ANN have become widely used for their ability to learn input–output relations by training from measured data. But it should be kept in mind that their performance is determined by the quality and the size of the training samples, as well as the suitability of the model used [9, 10]. Genetic algorithms present another possibility for non-linear identification, which can be especially useful for the purposes of parameter estimation in non-linear dynamic systems [9]. However, it should be noted that the last two techniques may be rather time-consuming.

The dynamic behaviour of robots is strongly influenced by the characteristics of their links. The robot connections are considered as one of the major sources of non-linearities in

the robot structure. As was mentioned, the dynamic behaviour of the robot elements and their vibration signals are clearly affected by the presence and the size of backlash and clearances in various robot links. The presence of a defect changes the signal coming from the joint. Thus, dynamic response signals are widely recognised and employed for purposes of condition monitoring and fault diagnosis. The presence of a defect introduces a non-linearity and leads to or influences the non-linear behaviour. Thus, a lot of non-linearity detection and identification approaches may be used for diagnosis and monitoring purposes. Condition monitoring, early defect detection, quantification, and evaluation in robot links are problems of utmost importance that receive increasing attention during the last years [14–26]. The non-linear behaviour makes the task of fault diagnosis and condition monitoring more difficult and more complicated.

There are two main types of condition monitoring methods—model- and non-model-based methods. Due to the complexity of the dynamics of robot joints as well as their highly non-linear behaviour, model-based condition monitoring procedures are rather difficult to develop. Accordingly, proper signal analysis, identification and classification methods are sought for condition monitoring and damage assessment in robotic structures. In general, the condition monitoring problem for a lot of non-linearly behaving systems has been approached by using different techniques, though signal and time series analysis methods are among the most commonly used ones. Signal-based diagnosis employs our physical understanding of the dynamic system behaviour in the presence of specific damage. Recently, a lot of authors apply the Hilbert transform signal processing technique for purposes of characterisation of non-linear vibrating systems [2, 7, 9]. This technique proved to be useful for purposes of defect detection in rotors [7]. Some authors suggest the use of spectrograms as well as different time–frequency transforms to detect defects and transient signals in gears and robotic devices [19, 20, 22]. These techniques can be combined with distance measures for the purposes of detection and with classification procedures for eventual quantification and/or localisation [22, 23]. Such methods are promising and easy to apply, but it should be kept in mind that their success is very much case dependent. The employment of signal model methods for non-linear systems, i.e. NARMAX or NARMAV methods, is based on an extension of the ARMA procedures for linear systems and presents a route towards model-based diagnosis [9, 14, 17]. Neural network and genetic algorithms are among the popular approaches which give a different perspective for diagnosis and identification of non-linear systems [13, 17, 24, 25]. Kalman and fault detection filters can create a powerful tool for defect detection and localisation when a dynamic model of the system is available. Some authors explore the feasibility of fuzzy sets theory for fault diagnosis purposes [2, 9]. Hypothesis testing, cluster analysis and pattern recognition techniques combined with signal processing procedures can constitute powerful approaches towards fault detection in non-linearly vibrating systems [7, 22–25]. Although non-model-based approaches prevail for a lot of condition monitoring problems, some authors suggest knowledge-based methods for fault diagnosis in industrial robots and manufacturing environment [14, 15, 16, 21]. Some studies offer a combination of knowledge-based approaches and signal processing techniques for fault diagnosis [7, 25].

However, it should be kept in mind that the application of the above listed methods is very much case dependent and most of them are developed and work for a special case of a non-linear system, as well as for a certain case of fault diagnosis.

This work attempts to introduce an alternative approach for modelling and condition monitoring of non-linearly behaving dynamic systems, which is suggested here for the dynamics of robot joints. The approach applies non-linear dynamics tools for the purposes of reconstruction of a model space, and employs some non-linear dynamics invariants for

the purposes of condition monitoring, instead of the traditional methods used in robot joints of dynamics [27].

3. EXPERIMENTS WITH INDUSTRIAL ROBOTS

Experiments were conducted on a PUMA 762 industrial robot (Fig. 1). The aim is to analyse the time response of some robot joints in the presence of a backlash and in normal condition (no backlash). For this purpose, various degrees of backlash were introduced in two joints of the robot (joint 4—wrist roll joint, and joint 6—wrist swivel joint) by adjusting the backlash screws of the robot links [19]. The joints are rotational and each of them is driven by a servomotor and gear transmission. The vibration responses are measured with an accelerometer mounted on the end transmission. Two series of experiments were performed—backlash in joint 6, and backlash in joint 4—zero (i.e. no backlash), small, medium and maximum backlash were introduced. The sampling frequency was 700 Hz and the duration of an observed block was 11 s.

Similar experiments were carried out on a two-link mechanism, each link driven by servomotor [19, 20]. Various static pre-loads were applied in order to simulate various degrees of backlash in the joint, namely no load, up to 11.8, 20–29.4 and 35–41.2 N. The first link is fixed and the second one is programmed to oscillate over a range of 0.125 rad from the vertical position. The acceleration responses are measured at the end of link 2 (Fig. 2).



Figure 1. Picture of the Puma robot.

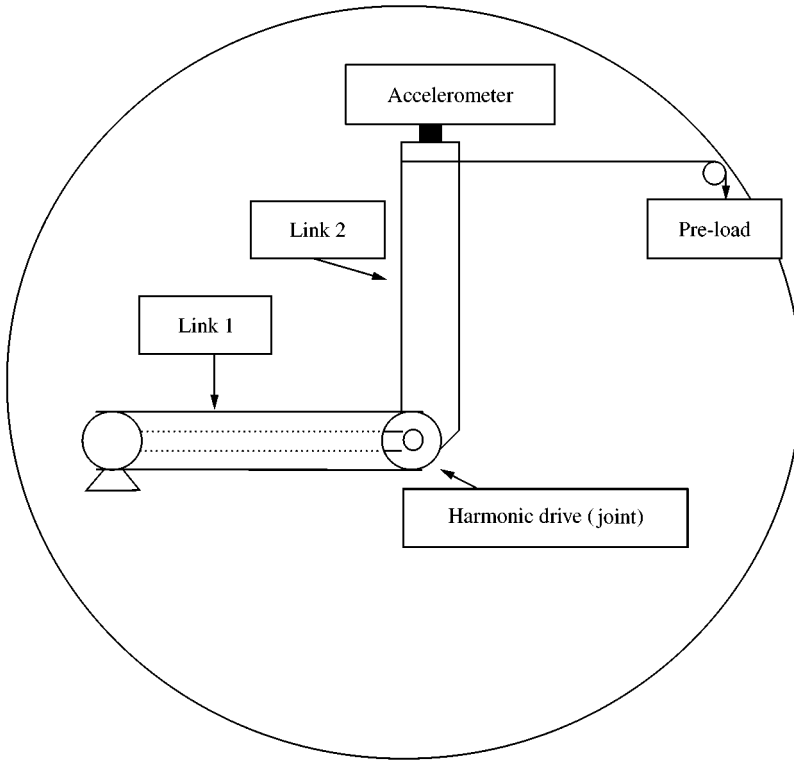


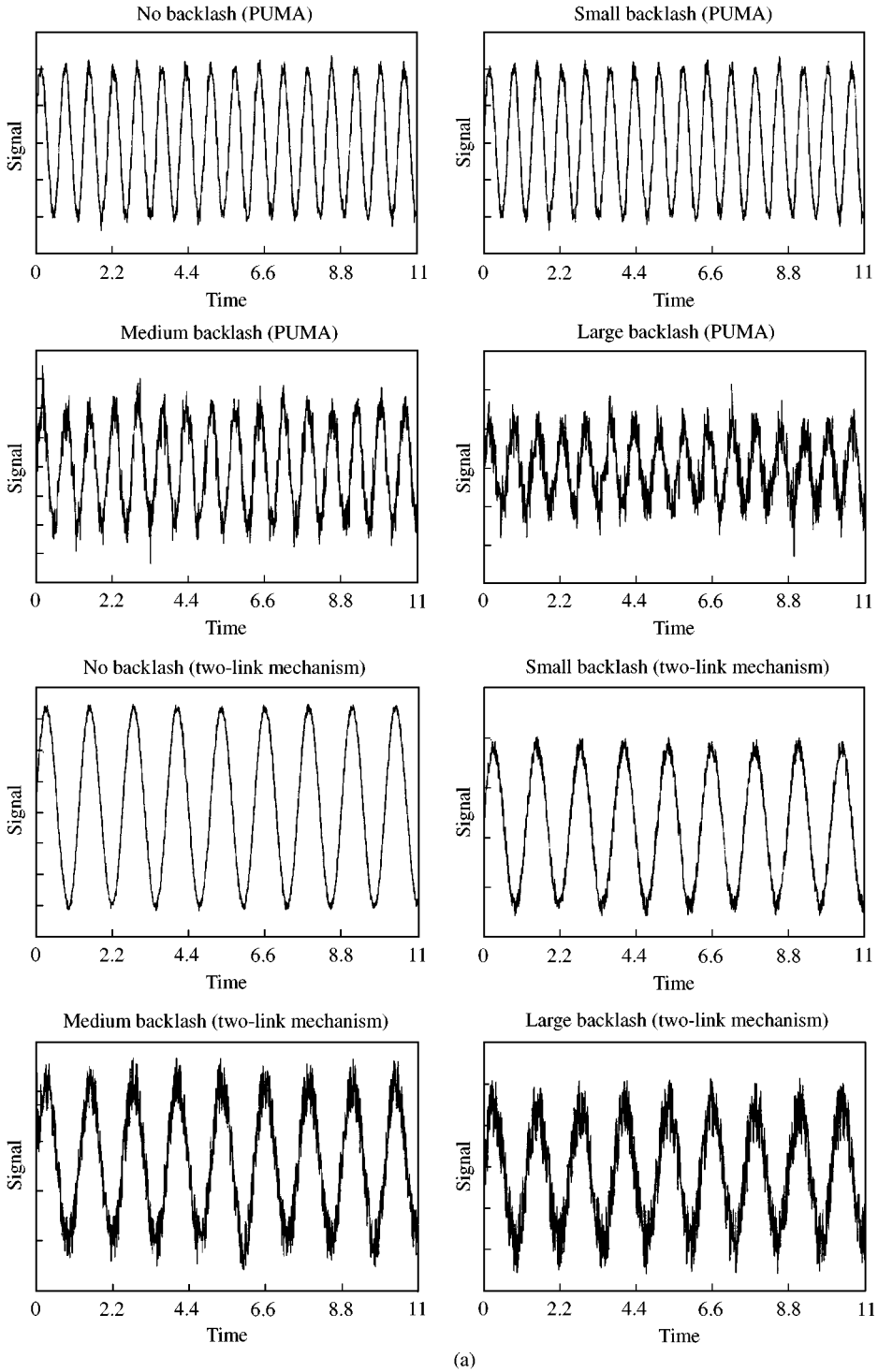
Figure 2. Two link mechanism.

4. SIGNAL ANALYSIS

In accordance with the experiments performed, and in correspondence with the joint type from which the signals come, we introduce four signal categories: no backlash signals (N), small backlash signals (S), medium backlash signals (M) and large backlash signals (L).

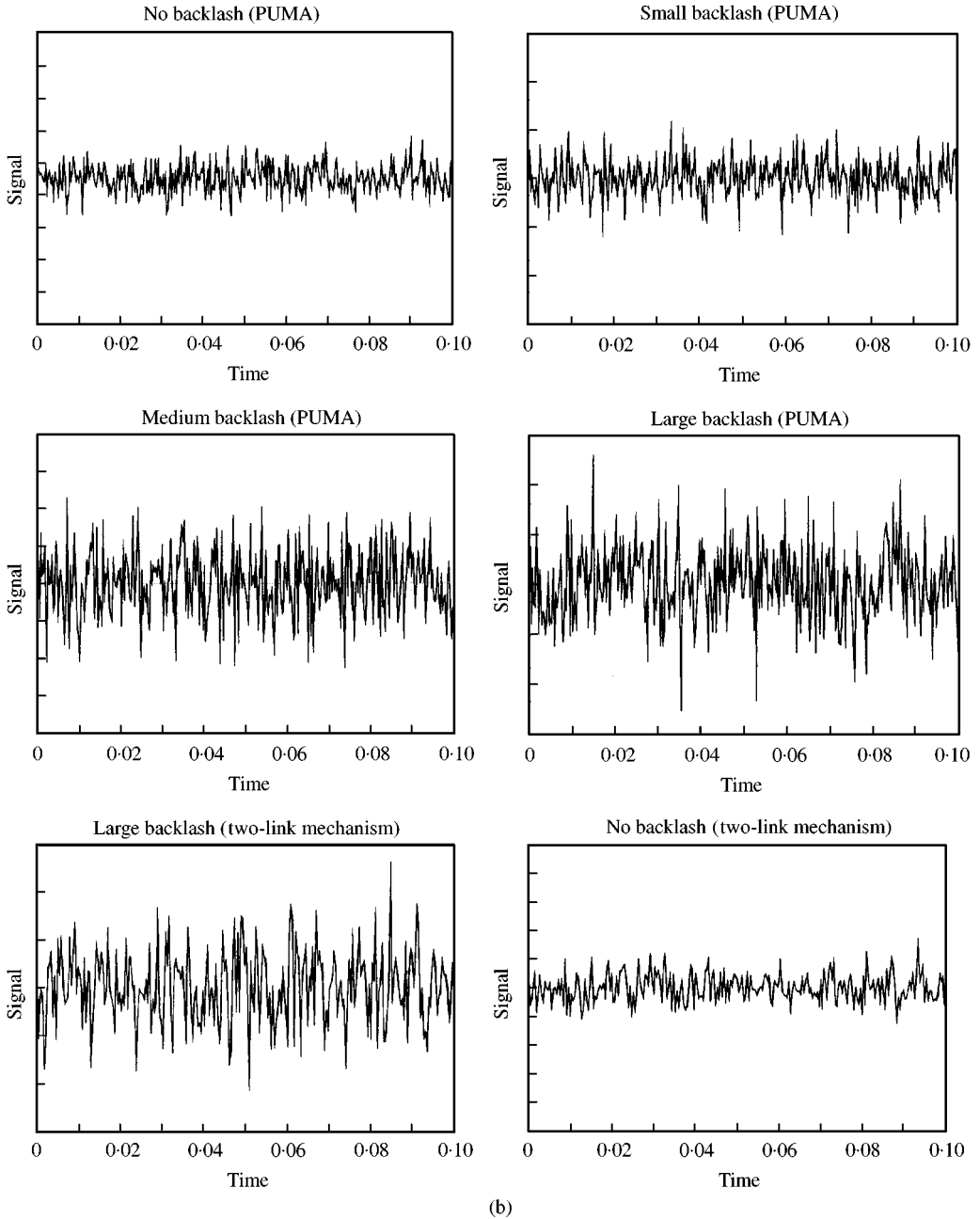
At first glance, the vibration signatures coming from the robot joints as well as those from the arm of the two-link mechanism seem very much periodic, since the joints rotate with constant frequency [Fig. 3(a)]. But obviously there is another component besides the periodic motion. Figure 3(b) shows a part of the first cycle of some signals after they were high-pass filtered in order to observe the non-periodic component of the motion. The visual appearance of the signals does not suggest any features to distinguish between signals coming from a damaged and a non-damaged link.

Some examples of the signal spectra are shown in Fig. 4. The spectra for the cases when backlash is present (especially for medium and maximum backlash) are somewhat different from those for no backlash. The situation with small backlash seems to be somewhat transitional. All the spectra are broadband. But for the N and some of the S series spectra, there are some distinct harmonics, which gradually disappear with the increase of the backlash size. The image of the transients as well as the spectra suggests that there could be a non-linearity that causes this behaviour. The next thing we try is the pseudo-phase-space representation [28, 29]. Without recovering the proper size of the time delay and the dimension of the embedding space, we plot the motion of the joints in a two-dimensional time delay space (trying several values of the time delay). The presumption is that the form



(a)

Figure 3. (a) Some typical signals. (b) Some typical transients.



(b)

Figure 3. (Continued)

of the plot will not change substantially, since the signal $x(t)$ $x(t + T)$ is related to the presentation (x, \dot{x}) and accordingly is expected to show similar properties. Thus the trajectories in $(x(t), x(t + T))$ are not expected to be closed curves if those in (x, \dot{x}) are not and the reverse. So, we expect the pseudo-phase-plane technique to preserve the major properties of the phase-space representation, and thus to enable us to draw some conclusions for the motion. We now look at the pseudo-phase-plane trajectories for the

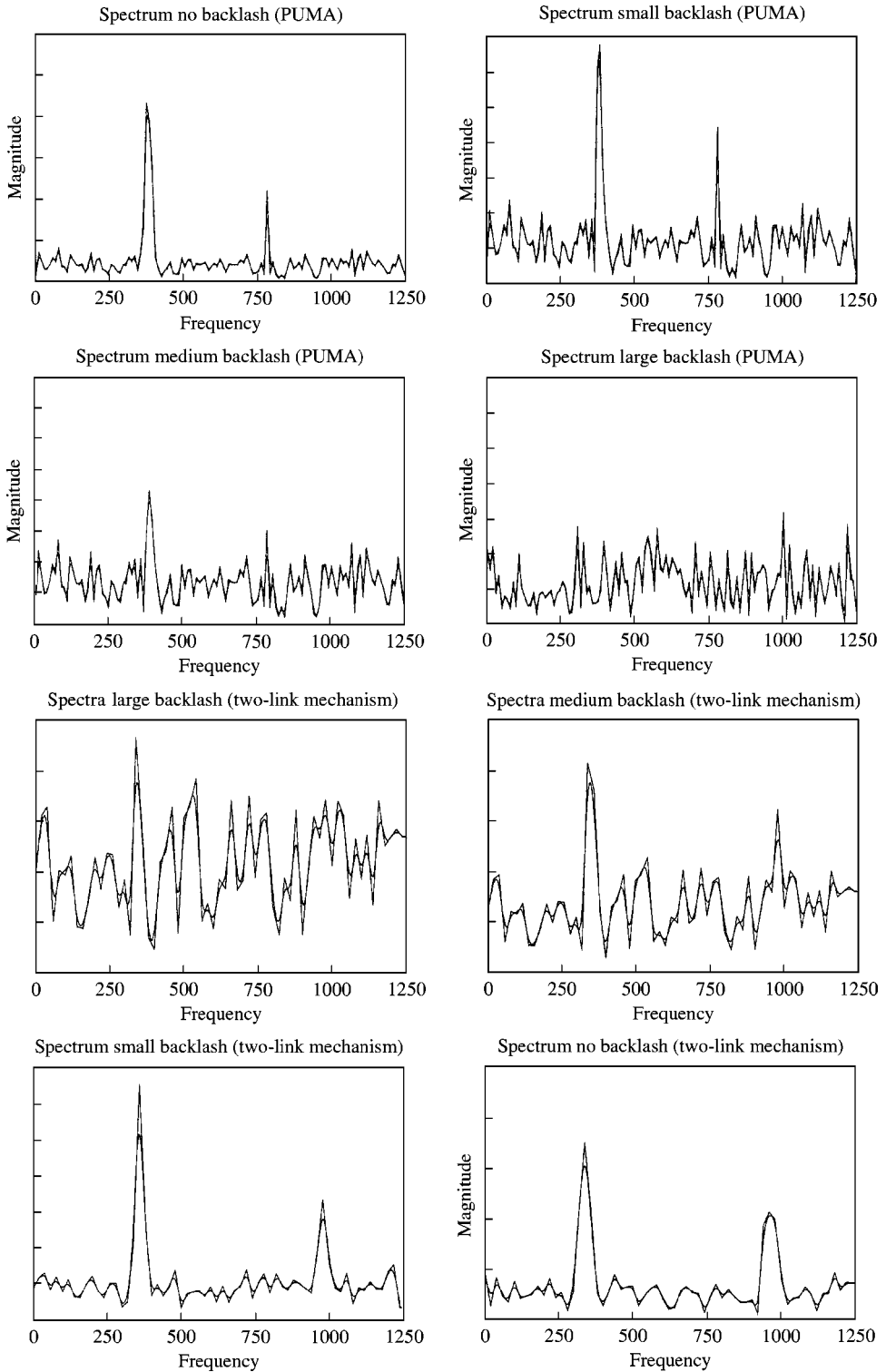


Figure 4. Some spectra.

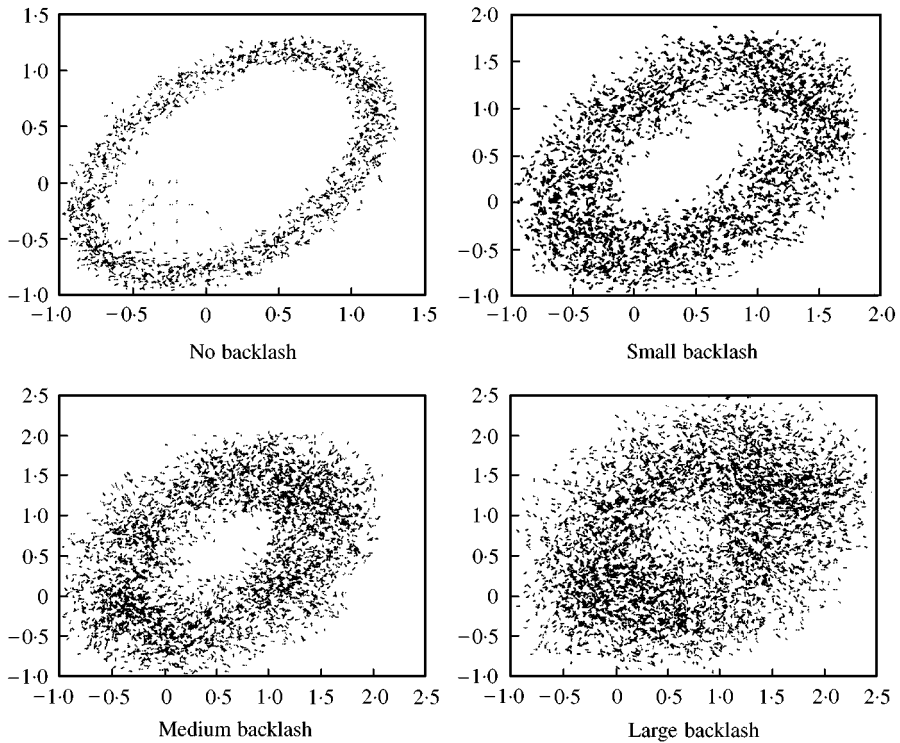


Figure 5. Typical pseudo phase space diagrams for different cases of backlash.

different signals that are shown in Fig. 5. The trajectories for the N and the S cases are between close curves and fractal points collections, which can suggest noise contaminated quasiperiodic motion or strange attractor in a low-dimensional space [28, 29–31]. Thus, one possible reason for such behaviour can be noise, and the other possible reason can be the presence of a weak non-linearity. Therefore, for the case of no backlash as well as for some cases of small backlash the evidence we have so far suggests either weak chaotic motion, or noise coloured quasiperiodic behaviour. A look at the pseudo-phase-plane trajectories for the M cases shows that they very much resemble fractal collection of points which can suggest chaotic motion to be represented in a low-dimensional phase space. This would justify a further attempt to project this motion in 3–4 time delay space. But again, this behaviour can result from noise coloured periodic or quasiperiodic motion. The phase-plane trajectories for the case of large backlash L assemble a fuzzy collection of points. This could imply either random behaviour or non-linear motion to be projected in a higher dimension phase space. Accordingly from the information we have so far, one cannot arrive at a unique conclusion for the dynamics of the categories of joints considered. It can be suggested that the introduction of a backlash in a robot joint leads to the increase of chaotic motion, which is weaker for the cases of smaller backlash and gets stronger the larger the backlash becomes. But it is not clear in any of the cases if noise (stochastic process) is not the cause for the observed behaviour. This is what we shall try to establish in the next sections. First, we shall recover the time lag and the embedding dimension of the space (Sections 4.1 and 4.2). That done, surrogate data tests will be used in order to check the hypotheses for the presence of non-linearities and of linearly correlated noise (Section 5).

5. RECONSTRUCTING THE PHASE SPACE

The first step towards modelling a motion is to find a space in which it can be projected accurately enough and with minimum or no loss of information. If one is to reconstruct a system dynamics from its time response, one such possibility is to recover its phase space made of delay coordinates, which is formally equivalent to the original (but unknown) space of the motion. In order to do that, the proper time lag T for the delay coordinates and the adequate dimension m of the space should be determined. In this phase space, the observation $S(t)$ is substituted by a vector $y(t)$

$$y(t) = [S(t), S(t + T), \dots, S(t + (m - 1)T)]. \quad (1)$$

For the purpose, a number of typical series from each category was selected. They are referred to as N (no backlash) S, M and L series (according to the categories introduced, see Section 4).

5.1. DETERMINING THE TIME LAG

The determination of the time lag is based on the idea of providing independent coordinates composed of the present observation $S(t)$, a subsequent view of the system $S(t + T)$ dynamically different from $S(t)$, etc., to produce the ingredients for a vector $y(t)$ defined according to equation (1). The notion of mutual information can be used for non-linear time series to determine the appropriate time delay parameter. The mutual information between two measurements represents the amount learned by one of the measurements about the other measurement. If the measurements are independent, then this amount is supposed to be zero. The mutual information for the measurements $S(t)$ and $S(t + T)$ is presented by

$$I(t, t + T) = \log_2 \frac{P(S(t), S(t + T))}{P(S(t))P(S(t + T))}. \quad (2)$$

The average mutual information between these two measurements will then be

$$I(T) = \sum_{S(t), S(t+T)} P(S(t), S(t + T)) \log_2 \frac{P(S(t), S(t + T))}{P(S(t))P(S(t + T))}. \quad (3)$$

It is expected that when T becomes large the measurements $S(t)$ and $S(t + T)$ will become independent, because of the chaotic behaviour of the signal, and thus $I(T)$ will tend to zero. It was suggested that the value of T for which the first minimum of the average mutual information occurs as a lag should be taken. The idea is that if the value of $I(T)$ decreases and goes to a minimum, the values of $S(t)$ and $S(t + T)$ will become more independent and the first minimum will be the minimum value for which they are independent. The choice of the first minimum of the average mutual information is analogous to the choice of the zero of the autocorrelation function for the linear case. It is expected (though it is not clear) that this choice, in analogy to the linear case, will provide the optimum value for T from the view point of predictability of $S(t + T)$ from knowledge of $S(t)$ [28, 32–34]. In any case, it works rather well for a lot of practical cases [29, 30] and we use this method to determine the time lag for the signals from robot joints.

Figure 6 shows some pictures of the relation $I(T)$ for the different cases considered. It can be observed that the value of the time lag that can be used for phase-space reconstruction for the different cases is different. In conclusion, one can derive that the values for the case of no backlash and the cases of small backlash show different values somewhat higher from those for the M and L cases. The time lag for the reconstruction of the time series for no

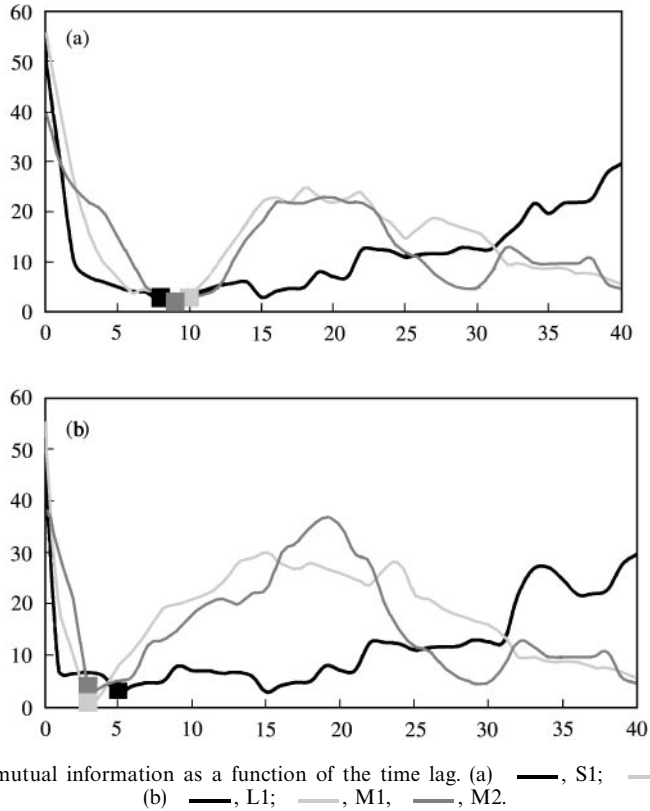


Figure 6. Average mutual information as a function of the time lag. (a) —, S1; —, N1, —, N2. (b) —, L1; —, M1, —, M2.

backlash and small backlash is between 8 and 10 (which is 80–100 μs), while it goes down to values of about 4–6 (40–60 μs), for the M and L series. This could be explained by the possible shorter time predictability for the cases of bigger backlash, when closer values are already independent, while equally distanced values for the cases of no backlash and small ones, are correlated.

It is worthwhile mentioning that the mutual information is directly connected to the non-linear properties of the source. It is also expected to be a rather robust characteristic in the case of contaminated measurements. The mutual information possesses a couple of attractive properties. It is easy to directly evaluate from the time series and it is invariant under smooth changes of the coordinate system. Thus, it is expected that the quantity $I(T)$ evaluated in time delay coordinates and in the original (but unknown) coordinates will have very much the same values. For these reasons, the mutual information will be used later to check for the presence of nonlinearities.

5.2. DETERMINING THE UNFOLDING DIMENSION OF THE PHASE SPACE

The next step is to recover the adequate number of coordinates m (the dimension) of the phase space. The number of coordinates m should provide a phase space with a dimension, in which the geometrical structure of the motion is completely unfolded, i.e. there are no hidden points, which cannot be projected in the space of the vector y [equation (1)].

The false nearest-neighbours techniques [28, 29, 32–34] can be used for the purpose. The idea of the method is to arrive at a dimension m for which there are no false neighbours that have come into the neighbourhood by a projection from a higher dimension. The method is

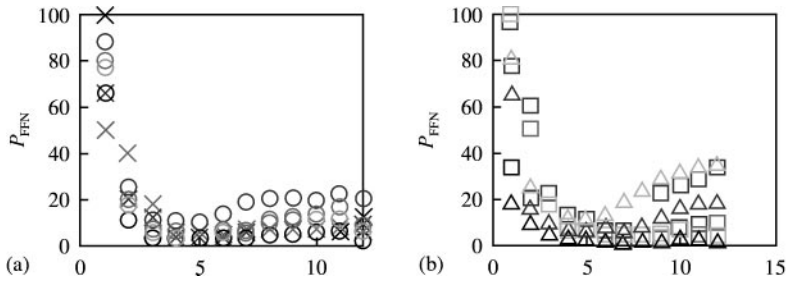


Figure 7. Percentage of false nearest neighbours, as a function of the space dimension m : (a) for N and S signals: \times N1; \times N2; \times N3; \circ S1; \circ S2; \circ S3; \circ S4 and (b) for M and L signals: \square M1; \square M2; \square M3; \square M4; \triangle L1; \triangle L2; \triangle L3.

used for the proper reconstruction of the phase space from the signal $S(t)$. When delay coordinates are used, the signal S is presented by a vector $\mathbf{y}(t)$ defined by (1), where T is the time delay suggested by the average mutual information method. For each point $\mathbf{y}(t)$, its nearest neighbour $\mathbf{y}^{NN}(t)$ in the m -dimensional space is found. If \mathbf{y} and \mathbf{y}^{NN} do not remain close enough as the dimension of the space is increased to $(m + 1)$, \mathbf{y}^{NN} is removed. Thus, increasing the dimension we gradually remove the false neighbours and decrease their number. The statistic of interest is the proportion of false nearest neighbours P_{FNN} . P_{FNN} should reach 0 when the sufficient embedding dimension is reached. In the case of noisy data P_{FNN} reaches its minimum, which is non-zero, and this value becomes higher, for data with higher noise contamination. Figure 7 gives some examples of how the percentage of false nearest neighbours decreases with the dimension. It can be observed that the percentage of nearest neighbours starts from 100 for both cases and gradually goes down, reaching its minimum for the values between 3 and 5. For some cases, this minimum is zero, but there are cases for which the minimum is not 0, the highest values being about 10%. For some signals the percentage of P_{FNN} stays 0 or maintains the minimal value it has reached, but for some signals it goes up again with the increase of the dimension. This should warn us for the presence of an additional ‘noise’ in these signals. There are such signals among the N and S signals as well as for the M and L signals [Figs 7(a) and (b)]. It should be observed that for most of the N and S signals, the minimum is reached for 3. Thus, one can conclude that for the cases of no backlash and small backlash a dimension of 3 or 4 will be enough to project the motion. For the cases M and L, the minimum is reached at about 5. Accordingly, a higher dimension will be required to unfold the motion for the cases of medium and large backlash. It should also be noted that for some M and L cases, the values after the minimum are kept rather high, some of them going up to above 30. Thus, for these cases we are left with the possibilities of noisy chaotic behaviour and the possibility of random motion, which are suggested by the behaviour P_{FNN} .

Thus, we have recovered the unfolding time delay state space for embedding the motion of robot joints from the considered categories. We have found a time lag of 8–10 (80–100 μ s) and a space dimension of $m_1 = 3$ (or 4) for N and S, and a time lag of 4–6 (40–60 μ s) and a space dimension of $m_2 = 5$ for the M and L signals. Accordingly, a signal $S(t)$ will be presented by a vector:

$$\mathbf{y}(t) = [S(t), S(t + T), \dots, S(t + m - 1)T]$$

where $m = m_1$ and a dimension of 4 should suffice for most of the N and S series, and $m = m_2 = 5$ for the M and L time series. But we still have to consider the possibility of random motion for all the time series—the nearest-neighbour method indicates that such a possibility exists.

6. DETECTING NON-LINEARITIES

In this section, we try to detect and prove the presence (or absence) of non-linearities in the considered joints from their time series response. This will answer the question as to whether the irregular behaviour of the joints is caused by non-linearity or by a random (stochastic) process. Surrogate data tests [27, 33, 31] are used for the purpose, which provide a rather general framework for investigating and characterising dynamic systems from their time response. The idea of these techniques is to make a hypothesis for the dynamic system and then to verify or reject it on the basis of certain statistics. The null hypothesis in this case will be that ‘the data produced is linearly correlated noise’. In the first step, the data are transformed in such a way that all structures except for the assumed properties is destroyed. Accordingly, a surrogate data set is generated, that mimics only the linear properties of the original time series. This is achieved by Fourier transforming the original time series and substituting the phases with random numbers. The power spectrum and the autocorrelation function are not affected by such a transform. Thus, after transforming back into the time domain, one gets a new time series with the same power spectrum. If the original data were just linearly correlated noise, by transforming it, we have not destroyed any underlying structure. On the contrary, if the data were generated by a non-linear system, then we have destroyed its invariants: Lyapunov exponents, dimensions, information and entropy characteristics, etc. Thus, a consequent estimation of any of the non-linear characteristics of the system should yield significant differences for the case of a non-linear system. Normally, to improve the robustness of the test, a number of surrogate data sets are generated and the mean value of the characteristic is compared to the original one [11, 12]. The original time series and the surrogate data sets are compared by using a discriminating test statistic. For this case, we used three discriminating statistics: the correlation dimension, the average mutual information, and the maximum Lyapunov exponent.

6.1. THE CORRELATION DIMENSION

The correlation dimension D_2 is the most frequently used statistic to characterise the geometric properties of the attractor. D_2 is computed as a limit of the correlation sum or the correlation integral [28–30, 34]:

$$D_2 = \lim_{r \rightarrow 0} \frac{\log|C(2, r)|}{2 \log|r|} \tag{4}$$

which counts all the points within distance r of each other. The correlation dimension is often used as a discriminating statistic in surrogate data tests, although it is sensitive to noise. For the test presented below, 25 iso-spectral lines were generated for each case considered, using the first 17 020 points. Figure 8 shows a number of correlation dimensions

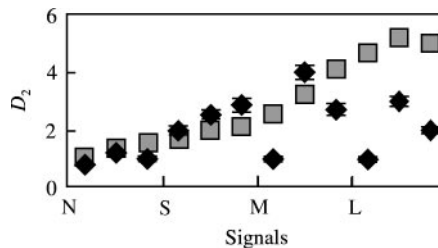


Figure 8. Correlation dimension for the original and the surrogate3 data series: ■, originals; ◆, surrogates.

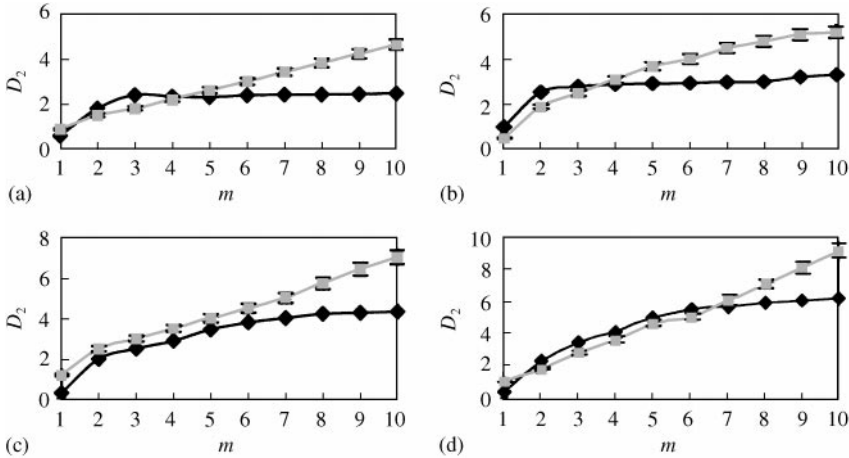


Figure 9. The correlation dimension for the original time series and the surrogates: (a) no backlash; (b) small backlash; (c) medium backlash; (d) large backlash: \blacklozenge —, originals; \blacksquare —, surrogates.

estimated for the original time series and the surrogates for all the cases considered. The surrogates are presented by the interval $E(D_{2S}) \pm 4\sigma_D$, where $E(D_{2S})$ is the mean value estimate for the surrogates and σ_D the standard deviation. For nearly all the cases, the values of the correlation dimension for the original series and the surrogates differ substantially. There are some cases from the N and S category signals for which the correlation dimensions D_2 for the original and the surrogate set are rather close. But then one can look at the correlation dimension as a function of the embedding dimension for both the original signals and the surrogate sets (Fig. 9). The behaviour of the lines $D_2(m)$ is apparently different for the original signals and the surrogates. A significance test with the statistics $z_D = (D_2 - E(D_{2S}))/\sigma_D/\sqrt{n}$, where $n = 25$ is the number of surrogates used for the test, at the level of significance of 5%, was also performed. The results are shown in Fig. 10(a). The values of the test statistics remain well below the significance level for all the cases considered. Hence, based on the above results, the null hypothesis can be rejected with a confidence level of 95%. Rejecting the null hypothesis means that the series do not result from linearly correlated noise, but this still does not imply a non-linear deterministic process. The source can be non-linearly correlated noise. Figure 9 shows convergence of the correlation dimension for the original time series, while there is no convergence for the surrogates. This implies a non-linear deterministic process. Thus, on the basis of the surrogate data test with the correlation dimension one should accept the hypothesis for a non-linear deterministic process with confidence level of 95%.

6.2. AVERAGE MUTUAL INFORMATION

Another test for non-linearities was performed by using the average mutual information, which was already defined and used to establish the proper time lag for recovering the embedding dimension [28, 29]. The mutual information between two measurements defines the amount learned by one of the measurements about the other. The average mutual information connects two sets of measurements with each other and establishes a criterion for their mutual dependence based on the idea of information connection. We took $S(t)$ as one of the measurement sets and $S(t + T)$ as the other measurement set. For a non-linear chaotic process, the average mutual information between these values is supposed to go to

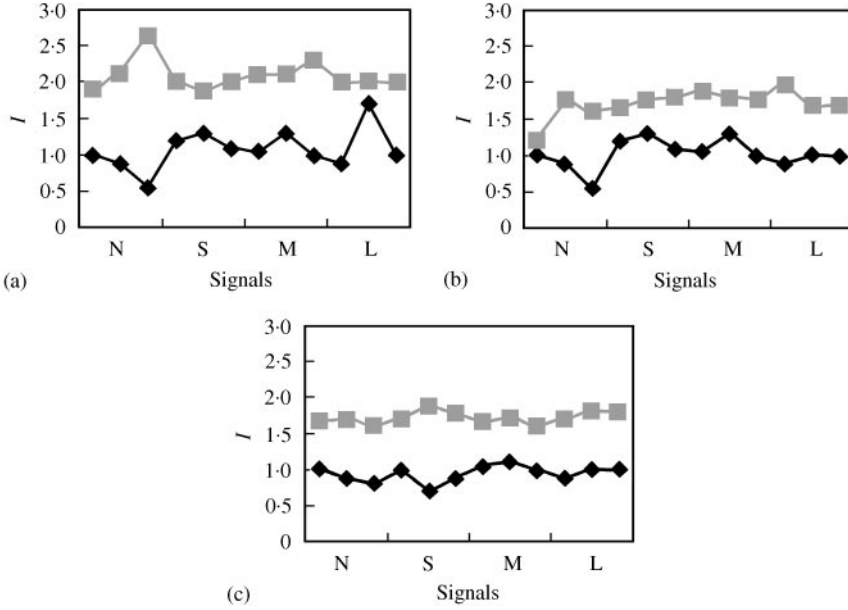


Figure 10. Results from the hypothesis testing (a) with the correlation dimension statistics z_D : —■—, significance level; —◆—, z_D statistics. (b) with the statistics z_a : —■—, significance level; —◆—, z_a statistics. (c) with the Lyapunov exponent statistics z_L : —■—, significance level; —◆—, z_L statistics.

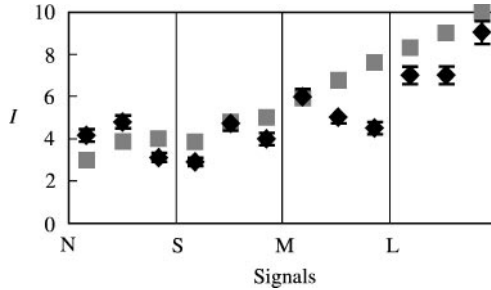


Figure 11. Averaged mutual information for the original time series and the surrogates: ■, originals; ◆, surrogates.

zero with increasing T since the chaotic behaviour of the signal makes them independent. The average mutual information $I(T)$ is also an invariant of the motion, which means that it does not change under smooth changes of the coordinate system, and thus it can be expected (similar to other invariants like the Lyapunov exponents and attractor dimensions) to be the same for the recovered time delay space and for the original (but unknown) space. On the other hand, in contrast to the autocorrelation function, which is tied to the linear properties of the signal source, $I(T)$ is connected to the non-linear properties of the signal. It has the advantages of being easily estimated and rather more insensitive to noise compared to the other invariants of the motion. Figure 11 shows the average mutual information for the original series and for the surrogates for several cases from all the categories of signals considered. The surrogates are shown by the mean value estimate $\pm 4\sigma_I$, where σ_I is the standard deviation. A test statistics was introduced with a significance level of 5%: $z_D = (I - E(I_s))/\sigma_I/\sqrt{n}$, where I is the average mutual information for the

original time series, $E(I_s)$ is the mean value of the average mutual information for the surrogate series, σ_I is its standard deviation and $n = 25$ is the number of surrogates used for the test.

Again it can be observed that the values for the original series and the surrogates differ substantially especially for the M and L series. There are only two cases that belong to N and S series for which the values of $I(T)$ are rather close, for all the other cases they are obviously different. Figure 10(b) shows the results from the significance test. It is easily observed that the values of the statistics of interest remain well below the significance level, which means that the null hypothesis can be rejected with a 95% confidence. Thus, using this statistics one can confirm the already obtained result, that time series produced by the robot joints, in the presence of a defect and without any defect, are not coloured noise.

6.3. MAXIMUM LYAPUNOV EXPONENTS

One more statistics was used to check the hypothesis for the presence of non-linearities in the dynamic behaviour of robot joints. We calculated the maximum Lyapunov exponent for the original series and the surrogate sets [28–30, 34]. The maximum Lyapunov exponent of a time series is a quantity that characterises the degree of chaoticity and the trajectory divergence of the motion. It is expected to be positive for the time series which comes from non-linear dynamic behaviour. Figure 12 shows the maximum Lyapunov exponents for the original series and the surrogates for all the considered types. For all the considered time series, there is an obvious difference in the values obtained for the original series and the surrogates. A hypothesis test with the following statistics: $z_\alpha = (\alpha - E(\alpha_s))/\sigma_\alpha/\sqrt{n}$, where $E(\alpha_s)$ and σ_α are the mean and the standard error of the α estimates for the surrogates, was also performed in order to reject the null hypothesis. The results for all the test cases are shown in Fig. 10(c). As can be observed, all the cases fall into the interval $z_\alpha \leq z_0$, where z_0 corresponds to the defined significance level of 5%. Therefore, on the basis of the test with the maximum Lyapunov exponent, the null hypothesis can be rejected for all the considered time series. On the other hand, the positive Lyapunov exponents for all the considered cases of joint motion and their increase from N towards the L cases, come to confirm the hypothesis for non-linear deterministic dynamic behaviour.

In this paragraph, we used three discriminating statistics and surrogate data tests in order to check the hypothesis that the time series produced by robot joint motion represent a deterministic non-linear process. The surrogate tests with all the statistics suggest the

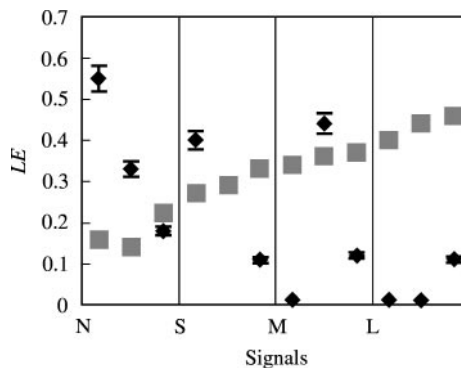


Figure 12. Maximum Lyapunov exponents for the originals and the surrogates: \blacksquare , originals; \blacklozenge , surrogates.

rejection of the null hypothesis for linearly correlated noise. The convergence of the correlation dimension with the embedding dimension and the positive Lyapunov exponents are used to reject the hypothesis for non-linear noise. Thus, from the performed tests, we come to the conclusion that signals from robot joints represent a deterministic non-linear process. The increase of the correlation dimension and the Lyapunov exponents from N towards L cases suggest the presence of a weak chaotic process when no backlash and small backlash is present which gets stronger for the M and L cases, i.e. with the increase of the backlash.

7. CHAOTIC DYNAMICS CHARACTERISTICS AND BACKLASH DETECTION AND CLASSIFICATION

As was already mentioned, backlash in robot joints can result in significant inaccuracies in the robot dynamics and performance and cause its inability for normal functioning. Here, we consider the problem for backlash detection and estimation in robot joints, using the already obtained results, employing some chaotic dynamics characteristics of the process. It was shown in the preceding paragraphs that the presence of a backlash in a robot joint can cause unstable chaotic behaviour. The previous results, presented in this paper, show that the degree of chaoticity is directly proportional to the backlash extent. The results for the maximum Lyapunov exponent and the correlation dimension for the different cases of backlash show that these characteristics tend to increase with the growth of the backlash.

In what follows, a possible procedure for backlash detection and classification that uses these characteristics is presented. In our experiments, the size of the backlash was controlled either by the adjustment of the backlash screws (for the PUMA robot) or by applying different pre-loads (for the two-link mechanism). Above, we have defined several categories of signals according to the backlash present in the joint, namely

- the category of signals from a no backlash joint N ,
- the category of signals from a joint with a small backlash S ,
- the category of signals from a joint with a medium backlash M and
- the category of signals from a joint with a large backlash L .

It is our aim to distinguish among these categories, extracting information directly from the measured vibration signals and making use of the recovered embedding dimension to estimate the characteristics of the corresponding time series. This can be achieved by using the above results, namely exploiting some non-linear dynamics characteristics of the signals.

As we already mentioned, the largest Lyapunov exponent of a signal characterises the degree of chaoticity of the system dynamics. A look at the Lyapunov exponents (LE) obtained for the different signal categories from both experiments (Fig. 12) convinces us that the maximum LEs vary for the different categories. They have the smallest values for the case of N signals increasing with the introduction and the growth of backlash. Consequently, the maximum Lyapunov exponents can be used as features to distinguish among the introduced categories. Figure 13(a) shows the ranges for the Lyapunov exponents for the different categories for both experiments. Another characteristic that can be observed to differ for the different categories is the correlation dimension. It is a geometric characteristic of the motion and gives an idea about the dimension of the attractor. It is also expected to increase with the increase of the degree of chaoticity. As can be observed (Fig. 8), our results suggest the same tendency as for the LE: the smallest correlation dimensions are registered for the N category and they increase with the increase of the backlash extent. Accordingly, one can try to use the correlation dimension also as a feature. Figure 13(b) shows the ranges of the correlation dimensions for the categories introduced. Thus, a very natural way to try

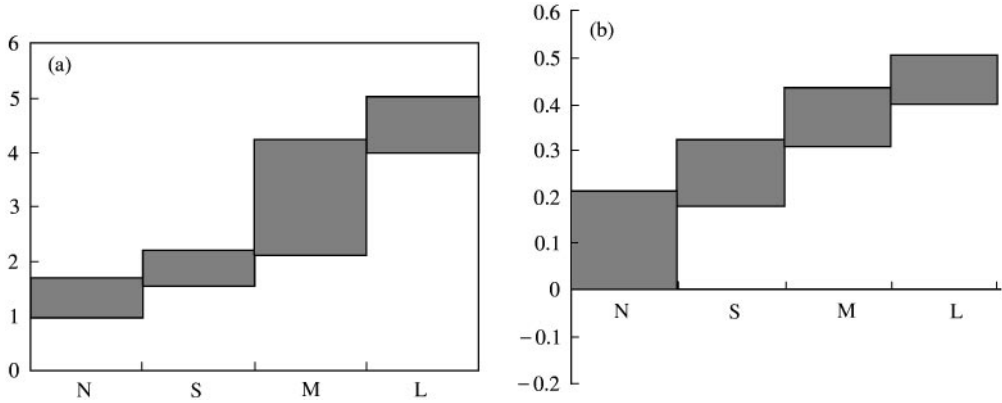


Figure 13. Ranges for (a) the correlation dimension, (b) the maximum Lyapunov exponents.

to distinguish among the considered categories is to develop a classifier using as features the maximum Lyapunov exponent and the correlation dimension. Instead of the signals S their Lyapunov exponent λ and the correlation dimension D_2 are used, thus forming a pattern vector \mathbf{s} for each signal

$$S \Rightarrow \mathbf{s} : \mathbf{s} = (\lambda, D_2)' \quad (5)$$

A rather simple classifier [2, 13–16], which can be used, is the one utilising the nearest-neighbour (NN) rule and the Euclidean distance as a dissimilarity measure. In order to build such a classifier, we take a prototype sample $\{\mathbf{s}_1, \mathbf{s}_2, \mathbf{s}_3, \dots, \mathbf{s}_n\}$ with known categorisation, i.e. each of the vectors \mathbf{s}_i belongs to one of the considered categories. The NN classifier categorises a test signal with a pattern vector \mathbf{x} to the category to which its nearest neighbour \mathbf{s}_j belongs, i.e.

$$\mathbf{x} \in I \quad \text{if } \mathbf{s}_j \in I \quad (6)$$

the nearest neighbour being the feature vector \mathbf{s}_j for which

$$D(\mathbf{s}_j, \mathbf{x}) = \min_i D(\mathbf{s}_i, \mathbf{x}) \quad (7)$$

where $D(\mathbf{y}, \mathbf{z})$ is the Euclidean distance between \mathbf{y} and \mathbf{z} . The NN classifier computes all the distances $D(\mathbf{s}_i, \mathbf{x})$, $i = 1, 2, \dots, n$. Then, according to the NN rule (6) the pattern \mathbf{x} is categorised to class I , if its nearest neighbour \mathbf{s}_j belongs to I , where \mathbf{s}_j satisfies equation (7) and I can take the values $I = \text{N.S.M.L}$. The same classifier can be used in order to detect backlash. In such a case, one introduces only two categories—no backlash (N) and backlash (B), where the B category joins the S.M. and L. categories. A joint will be considered damaged (with a backlash) if its nearest neighbour belongs to the B category, and it will be considered non-damaged if its nearest neighbour belongs to the N category.

This makes a rather simple damage detection classification algorithm:

- (1) The pattern vector \mathbf{x} of the signal is computed.
- (2) Its distances $D(\mathbf{s}_i, \mathbf{x})$, $i = 1, 2, \dots, n$ to all the feature vectors from the prototype sample $\{\mathbf{s}_1, \dots, \mathbf{s}_n\}$ are calculated.
- (3) The minimum $D(\mathbf{s}_j, \mathbf{x}) = \min_i D(\mathbf{s}_i, \mathbf{x})$ of the distances of x to the prototype vectors $\{\mathbf{s}_1, \dots, \mathbf{s}_n\}$ is found.

TABLE 1
Confusion matrices for the classifiers

(a) To classify backlash

	N	S	M	L
True class N	92	7	1	0
True class S	7	91	2	0
True class M	0	1	93	6
True class L	0	0	5	95

(b) To detect backlash

	N	B
True class N (no backlash)	92	8
True class B (backlash)	2	98

(4) If $s_j \in B$, then the signal is categorised to the backlash category B.

(5) If $s_j \in N$, then the signal is categorised to the no-backlash category N.

A similar classification algorithm can be organised for the case of four classes N, S, M, L.

The developed procedure was applied by using data from both experiments considered. Two classifiers are built by using signals measured from the PUMA robot joints and the two-link mechanism—one that distinguishes between backlash and no backlash joints (backlash detection classifier) and another one that recognises among N, S, M and L joints (backlash quantification classifier). These classifiers were then applied to categorise signals recorded from both experiments. This was made possible by the fact that the features for signals recorded from both types of experiments vary in the same ranges (Fig. 13).

For this study, 139 signals (35 of them from the N category, 33 from S, 36 from M and 35 from L) and 151 signals (38 from N, 38 from S, 38 from M and 37 from L), each one containing about 3000 points, were measured from the PUMA robot axes and from the two-link mechanism, respectively, to form the prototype sample s_j of feature vectors with known categorisation. Then, the performance of the developed classifiers was checked with another test sample of signals (96 signals from the PUMA robot axes and another 96—from the two-link mechanism, i.e. 24 from each category were measured with each experimental set-up). Tables 1(a) and (b) summarise the results for the performance of the classifiers. The numbers on the main diagonals of Tables 1(a) and (b) give the total percentage (for both experiments) of correctly classified signals for the quantification classifiers and the detection classifiers, respectively. For instance, the number on the N row and the N column (NN) of Table 1(a) gives the total percentage of N signals that were correctly classified as N signals. The figures outside the diagonal give the total percentage of the incorrectly classified signals, i.e. the number on the N row and the S column (NS) of Table 1(a) gives the amount of the N signals incorrectly classified as S (small backlash) signals. In general, the classifiers demonstrate rather good performance in distinguishing among the different signal categories. There is a certain confusion between signals from neighbour classes, i.e. N and S, M and L [see elements NS and SN and elements ML and ML from Table 1(a)]. This could be due to overlapping in the initial signal categories as well as noise in the measured signals. Both of these might lead to close or even the same features for vectors from different classes, which will result in overlapping of the neighbouring classes. Such an effect can be observed

in the ranges for the features [Figs 13(a) and (b)]—they are somewhat overlapping. When the same classifier is used as a backlash detector only i.e. to recognise between no backlash and backlash joints, the detectability of the backlash category is rather better than that for the no backlash category [Table 1(b)]. This can be attributed to the fact that in this case the prototype sample s_j contains much more signals from the backlash category compared to those from the no backlash one, thus increasing the *a priori* probability of the backlash class.

8. SOME CONCLUSIONS AND DISCUSSION

Robot dynamics analysis is an extremely difficult and challenging area. It has attracted and attracts a lot of attention because of the importance to have an accurate enough model to predict robot joints motion on the one hand and the difficulties to develop such a model on the other. It is very difficult and in some cases even impossible to take into account all the phenomena and the interactions that affect a robot joint motion besides the governing rigid body equations hence, the difficulties to create an accurate enough analytical model. The introduction of a defect makes the task still more complicated, since it introduces an additional non-linearity in the robot joint. In this paper, the dynamics of robot joints in the presence of backlash and in the no backlash case is analysed using an alternative approach making use of their acceleration measurements in the time domain, employing non-linear dynamics tools and time series analysis. The following categories of signals are considered—(i) signals from a no backlash joint, (ii) signals from a joint with a small backlash, (iii) signals from a joint with a medium backlash and (iv) signals from a joint with a large backlash. Experimentally, these categories are introduced by adjusting the backlash screws of the joint for the PUMA robot case or by applying different pre-loads for the two-link mechanism. The average mutual information is used to reconstruct the time delay for several cases from each category. Our results showed that the time delay parameter is smaller for the cases of medium and large backlash and it grows for the small and no backlash cases. The false nearest-neighbour technique is applied to find the minimal embedding dimension for the considered time series, which proved to be smaller for the case of no and small backlash, and a bit larger for the medium and large backlash cases. The embedding dimension and the maximum Lyapunov exponents proved to be directly proportional to the backlash size, thus implying smaller predictability for the cases with a bigger backlash and more regular (periodic) behaviour for the cases of small and no backlash. The decrease of the time delay parameter with the backlash growth suggests the same tendency in the behaviour. These results imply that in spite of the harmonic motion performed by the joint, there is another component, which could be a non-linear deterministic process. But there still exists the possibility of random noise, added to the harmonic motion of the joint. One of these hypotheses has to be rejected. Surrogate data tests with several test characteristics were applied in order to check for non-linearities in the considered time series. The hypothesis for linearly correlated noise was rejected for all the time series types on the basis of all the test statistics used. The possibility for non-linearly correlated noise was also rejected on the basis of the convergence of the correlation dimension and the positive maximum Lyapunov exponents for the original series. Thus we characterise all the considered time series as a combination of periodic and non-linear, chaotic, behaviour. The hypothesis for chaoticity is confirmed by the Lyapunov exponents of the time series—they turned out positive for all the considered time series, except for some N series (for nearly all the backlash cases the maximum LEs are non-negative and less than 1). This suggests the presence of a weak chaotic process and implies small unpredictability for cases of no and small backlash. The tendency for increase of the largest Lyapunov

and the correlation dimension, as well as the embedding dimension with the increase of the backlash size confirms the hypothesis for slowly growing chaoticity with the increase of the backlash extent. Nevertheless, the chaoticity and the unpredictability of the motion remain small for all the considered cases, including those of large backlash (all the maximum LEs do not exceed 1).

The presence of a non-linearity, which causes the irregular (unstable) component of the robot joint motion, suggests the possibility for recovering a deterministic non-linear model in the phase space to describe the dynamics of robot joints especially in the presence of a defect. The reconstruction of the embedding phase space is the first step towards creating a model in the time delay space. Such a model should connect some characteristics featuring the present defect, i.e. its type, size, etc., to the non-linear dynamics characteristics. The results for the Lyapunov exponents and the correlation dimension show different values for the different categories, as well as a tendency for increase with the backlash growth. This also implies the existence of a relationship between the backlash size and the chaotic invariants. Obtaining such kind of a model will open a route towards solving condition monitoring and backlash detection problems using identification tools.

This work offers a classification procedure that is used for backlash detection and classification. The Lyapunov exponents and the correlation dimension show a tendency to differ for the different categories introduced. Accordingly, their values are used as features to distinguish among the considered backlash categories. Classifiers, which work on an NN principle, are developed by using the data from both experiments. The performance of the classifiers is tested with another set of signals, obtained from the PUMA robot and the two-link mechanism. They show very good performance in distinguishing among the introduced backlash categories as well as for backlash detection. Hopefully, other non-linear dynamics characteristics can also be used, that are more easily obtained and more representative for the different signal types, in order to facilitate and improve the procedure. A look at the pseudo-phase-space representations can suggest the use of some geometric characteristics of the attractor as characteristic features.

It is expected that the same approach may be applied when other defects are present in the robot connections, as well as for the purposes of analysis and modelling of different non-linear effects that influence the motion of robot joints (friction, non-linear materials, flexibility, etc.). The non-linear dynamics approach not only provides a tool for condition monitoring and fault detection in robot joints, it could prove to be a valuable tool for the analysis of the motion of robot joints. Furthermore, it might provide a route towards alternative modelling of the motion of robot joints in the presence of non-linear effects and faults, which are known to have a considerable influence on the robot dynamics and their performance. This in its turn will open possibilities towards the estimation and control of robot motion, accounting for such non-linear effects, making use of inverse identification and optimisation methods.

This work presents just a beginning in the application of non-linear dynamics for modelling and analysis of robot joints motion in the presence of non-linearities as well as for condition monitoring and control purposes.

REFERENCES

1. G. TOMLINSON 1987 *Proceeding of the Fifth International Modal Analysis Conference, London*. Detection, identification and quantification of nonlinearity in modal analysis—a review.
2. K. WYCKAERT 1992 Development and evaluation of detection and evaluation schemes for the nonlinear dynamical behaviour of mechanical structures. *Ph.D. thesis, Department of Mechanical Engineering, Katholieke Universiteit Leuven, PMA, March*.

3. G. TOMLINSON and J. HIBBERT 1979 *Journal of Sound and Vibration* **64**, 64–78. Identification of the dynamic characteristics of a structure with Coulomb friction.
4. R. FILLOD, G. LALLEMENT and J. PIRANDA 1984 *Proceedings of the Second International Modal Analysis Conference, Orlando*. Is a structure nonlinear? If yes, how to perform its modal identification.
5. I. TRENDAFILOVA, V. LENAERTS, G. KERSCHEN, J-C. GOLINVAL, H. VAN BRUSSEL and W. HEYLEN 2000 *Proceedings of the 25th International Seminar Modal Analysis, Leuven, Belgium*. Detection, localization and identification of nonlinearities in structural dynamics.
6. D. E. ADAMS and R. J. ALLEMANG 1999 *Journal of Vibration and Acoustics* **121**, 495–500. Characterization of nonlinear vibrating systems using internal feedback and frequency response modulation.
7. M. FELDMAN and S. SEIBOLD 1999 *Journal of Vibration and Control* **5**, 421–442. Damage diagnosis of rotors: application of Hilbert transform and multihypothesis testing.
8. X. MA, M. F. A. AZEES and F. VAKAKIS 2000 *Mechanical Systems and Signal Processing* **14**, 37–48. Non-linear normal modes and non-parametric system identification of nonlinear oscillators.
9. K. WORDEN 2000 *Proceedings of European COST F3 Conference System Identification & Structural Health Monitoring, Madrid*. Nonlinearity in structural dynamics—the last ten years.
10. J. LEE and B. KRAMER 1994 *Journal of Manufacturing Systems* **12**, 428–435. Analysis of machine degradation using a neural network base pattern discrimination model.
11. K. WORDEN and G. R. TOMLINSON 1993 *Mechanical Systems and Signal Processing* **8**, 319–356. Modelling and classification of nonlinear systems using neural networks. Part I: simulation.
12. K. WORDEN, G. R. TOMLINSON, W. LIM and G. SAUER 1993 *Mechanical Systems and Signal Processing* **8**, 395–419. Modelling and simulation of nonlinear systems using neural networks. Part II: a preliminary experiment.
13. K. WORDEN, A. D. BALL and G. R. TOMLINSON 1993 *Smart Materials and Structures* **2**, 189–200. Fault location in a framework structure using neural network.
14. R. ISERMAN 1993 *Automatica* **29**, 815–835. Fault diagnosis of machines via parameter estimation and knowledge processing—Tutorial paper.
15. K. CHUNG and J. TOU 1992 *Mechatronic Systems Engineering* **1**, 262–292. Knowledge based approach to fault diagnosis and process control in automated manufacturing Environment.
16. B. FREYERMUTH 1991 *Proceedings of 1991 IEEE International Conference Robotics and Automation, Sacramento, California*. An approach to model based fault diagnosis of industrial robots.
17. P. FINK and J. LUSTH 1987 *IEEE Transactions on Systems, Man and Cybernetics* **SMC-17**, 38–49. Expert systems and diagnostic expertise in the mechanical and electrical domains.
18. J. MATHEW 1997 *Proceedings of the Fifth International Congress Sound and Vibration Adelaide, South Australia*, 903–918. Some recent advances in signal processing for vibration monitoring.
19. M.-CH PAN, H. VAN BRUSSEL, P. SAS and B. VERBEURE 1996 *ISMA 19—Tools for Noise and Vibration* 407–421. Detection and quantification of the link-joint backlash of a robot- time-frequency signal representation and feature extraction.
20. M.-CH PAN, H. VAN BRUSSEL, P. SAS and B. VERBEURE 1998 *Transactions of ASME, Journal of Vibration and Acoustics* **120**, 13–24. Fault diagnosis of joint backlash.
21. J. STEIN and CH-H. WANG 1998 *Journal of Dynamic Systems, Measurement and Control, Trans ASME* **120**, 211–233. Estimation of gear backlash: theory and simulation.
22. I. TRENDAFILOVA, H. VAN BRUSSEL and B. VERBEURE 1999 In *Identification in Engineering Systems, Proceedings of the II International Conference*, M. I. Friswell, J. E. Mottershead and A. Lees (eds), 169–178. On feature extraction for condition monitoring using time series analysis and distance techniques.
23. I. TRENDAFILOVA, H. VAN BRUSSEL and B. VERBEURE 2000 *Inverse Problems in Engineering* **8**, 1–24. On feature extraction for condition monitoring using nonlinear time series analysis and pattern recognition procedures.
24. K. WORDEN, G. MANSON, J. N. R. FIELLER and S. CURTIS 1998 *Proceedings of ISMA 23, Noise and Vibration Engineering Conference, Leuven, Belgium*, 73–79. Damage detection using multivariate statistics, Part I: outlier analysis.
25. S. WANG *Proceedings of the First International Machinery Monitoring and Diagnostics Conference, Las Vegas, NV*, 516–522. AI and expert systems for diagnostics.
26. G. T. ZHENG and MCFADDEN 1999 *Transactions of ASME* **121**, 328–333. A time frequency distribution for analysis of signals with transient components and its application to vibration analysis.

27. C. GANSEMN 1998 *Ph.D. thesis, Division PMA*, K. U. Leuven. Dynamic Modeling and identification of mechanisms with application to industrial robots.
28. H. ABARBANEL 1996 *Analysis of observed chaotic data*. Berlin: Springer-Verlag.
29. H. KRANTZ and T. SCHREIBER 1997 *Nonlinear Time Series Analysis*. Cambridge: Cambridge University Press.
30. F. MOON 1987 *Chaotic Vibrations. An Introduction for Applied Scientists and Engineers* New York: John Wiley & Sons Inc.
31. M. PALUS 1995 *Physica* **D80**, 186–205. Testing for nonlinearities using redundancies: quantitative and qualitative aspects.
32. A. M. FRASER and H. L. SWINNEY 1986 *Physica* **A33**, 1134–1140. Independent coordinates for strange attractors from mutual information.
33. J. GRADISEK, E. GOVEKAR and I. GRABEC 1998 *Mechanical Systems and Signal Processing* **12**, 839–854. Time series analysis in metal cutting: chatter versus chatter-free cutting.
34. R. HILBORN 1994 *Chaos and Nonlinear Dynamics*. Oxford: Oxford University Press.
35. J. THEILER, S. EUBANK, A. LONGTIN, B. GALDRIKIAN and J. FARMER 1992 *Physica* **D 58**, 77–94. Testing for nonlinearity in time series: the method of surrogate data.
36. J. TOU and R. GONZALES 1978 *Pattern Recognition Principles*. Reading, MA: Addison-Wesley Publ. Comp.
37. K. FUKUNAGA 1990 *Introduction to Statistical Pattern Recognition*. New York: Academic Press.